

18. J. Wolfgang, S. M. Risser, S. Priyadarshy, D. N. Beratan, *J. Phys. Chem.* **101**, 2986 (1997).
19. I. Daizadeh, E. S. Medvedev, A. A. Stuchebrukhov, *Proc. Natl. Acad. Sci. U.S.A.* **94**, 3703 (1997).
20. S. Priyadarshy, S. Skourtis, S. M. Risser, D. N. Beratan, *J. Chem. Phys.* **104**, 9473 (1996).
21. I. A. Balabin and J. N. Onuchic, *J. Phys. Chem.* **100**, 11573 (1996).
22. P. Dauber-Osguthorpe et al., *Proteins Struct. Funct. Genet.* **4**, 31 (1988).
23. Larger nuclear motions, which we do not allow here, may even change the tube structure, leading to more pronounced dynamical effects.
24. A. Kuki and P. G. Volynes, *Science* **236**, 1647 (1987).
25. S. S. Skourtis and D. N. Beratan, *J. Phys. Chem.* **101**, 1215 (1997).
26. The mediating role of Trp^{M252} has been suggested in M. Plato, M. E. Michel-Beyerle, M. Bixon, J. Jortner, *FEBS Lett.* **249**, 70 (1989).
27. S. Priyadarshy, S. M. Risser, D. N. Beratan, *J. Biol. Inorg. Chem.* **3**, 196 (1998).
28. W. B. Curry et al., *J. Bioenerg. Biomembr.* **27**, 285 (1995).
29. C. C. Page, C. C. Moser, X. Chen, P. L. Dutton, *Nature* **402**, 47 (1999).
30. I. A. Balabin and J. N. Onuchic, *J. Phys. Chem.* **102**, 7497 (1998).
31. We thank G. Feher, M. Okamura, and D. Beratan for valuable discussions. Funded by NIH (grant no. GM48043).

30 May 2000; accepted 16 August 2000

Xenon as a Complex Ligand: The Tetra Xenono Gold(II) Cation in $\text{AuXe}_4^{2+}(\text{Sb}_2\text{F}_{11}^-)_2$

Stefan Seidel and Konrad Seppelt*

The first metal-xenon compound with direct gold-xenon bonds is achieved by reduction of AuF_3 with elemental xenon. The square planar AuXe_4^{2+} cation is established by a single-crystal structure determination, with a gold-xenon bond length of approximately 274 picometers. The bonding between gold and xenon is of the σ donor type, resulting in a charge of approximately 0.4 per xenon atom.

Since the creation of the first noble gas compound, XePtF_6 , in 1962 (1), xenon compounds with direct bonds to fluorine, oxygen, nitrogen, carbon, xenon itself, and most recently, chlorine, have been established, with the list for krypton-bonded elements being much shorter. All these bonded atoms are electronegative main-group elements. Noble gas chemistry would be greatly enhanced if xenon (or other noble gases) could be bonded directly to metal atoms or ions.

There have been indications that metal-xenon bonds can be formed. In noble gas matrices, the complexes $(\text{CO})_5\text{Mo} \dots \text{Xe}$, $(\text{CO})_5\text{W} \dots \text{Kr}$, $(\text{CO})_5\text{Mo} \dots \text{Kr}$, and $(\text{CO})_5\text{Fe}^+ \dots \text{Kr}$ (2) have been detected. In supercritical Xe and Kr solutions, short-lived transients containing xenon or krypton metal bonds have been observed many times (3). The Au-Xe^+ ion has also been detected by mass spectroscopy, and has been calculated with a best estimate for the bond distance of 257 pm and of $30 \pm 3 \text{ kcal mol}^{-1}$ for the bond energy (4). Even Ar-AuCl and Kr-AuCl have been observed by microwave spectrometry (5). It is also possible that a similar complex between platinum fluoride(s) and xenon was an intermediate in the seminal 1962 preparation of the first xenon compound, which was formed using elemental xenon and PtF_6 (1). To this day, the exact nature of the product of that reaction has not been determined (6).

The original goal of this study was the preparation of the elusive gold(I) fluoride, AuF , via the reduction of AuF_3 with a weakly coordinating agent. The reaction between AuF_3 and AsF_3 in HF/SbF_5 solution afforded $\text{F}_3\text{As-Au} \dots \text{F} \dots \text{SbF}_5$, the first derivative of AuF (7). We then replaced AsF_3 with xenon as a very mild reducing and very weakly coordinating agent, in order to reach AuF . The reaction, however, stopped at the Au^{2+} state and resulted in a completely unexpected complex, the cation AuXe_4^{2+} , of which dark red crystals can be grown at -78°C . Removal of gaseous xenon under vacuum results in the crystallization of $\text{Au}(\text{SbF}_6)_2$, one of the few true Au^{2+} salts that are known (8). Addition of Xe to Au^{2+} in HF/SbF_5 gives a dark red solution at -40°C . Because the reaction between Au^{2+} and Xe is reversible, a xenon pressure of about 10 bar (1000 kPa) is necessary to stabilize AuXe_4^{2+} in solution at room temperature.

A single-crystal structure determination revealed the existence of $\text{AuXe}_4^{2+}(\text{Sb}_2\text{F}_{11}^-)_2$ (9). The cation forms a regular square, with Au-Xe bond lengths ranging from 272.8(1) to 275.0(1) pm. Three weak contacts between the cation and the anion complete the coordination sphere around the gold atom with $\text{Au} \dots \text{F}$ distances of 267.1 and 315.3 pm (Fig. 1). Shortest contacts between xenon and fluorine atoms are all about 310 pm long. The structure of the anion $\text{Sb}_2\text{F}_{11}^-$ appears quite normal. The compound is stable to about -40°C . Warming above this temperature results in liquidification, loss of gaseous xenon, and a dramatic color change from dark red to light orange.

The compound $\text{AuXe}_4^{2+}(\text{Sb}_2\text{F}_{11}^-)_2$ has

also been characterized by Raman spectroscopy. In addition to bonds that are typical of the $\text{Sb}_2\text{F}_{11}^-$ anion, a very strong band is observed at 129 cm^{-1} . This is assigned to the totally symmetric stretching vibration of the AuXe_4^{2+} , on the basis of the prediction of this band at $\sim 100 \text{ cm}^{-1}$ by a number of ab initio and density functional theory calculations (Table 1) (10).

The calculations all predict Au-Xe bond lengths a little longer than the experimental value. The mean bond energy with respect to Au^{2+} and 4 Xe is calculated to be approximately $200 \text{ kcal mol}^{-1}$ (Table 1). This value is reasonable considering the thermal behavior of the compound $\text{AuXe}_4^{2+}(\text{Sb}_2\text{F}_{11}^-)_2$. In the complex, xenon functions as a σ donor toward Au^{2+} . This is reflected in the calculated charge distribution within the cation, where the main part of the positive charge resides on the xenon atoms. Gold is the most electronegative transition element known, in part due to the strong relativistic effect (11). This may explain the large charge transfer.

In principle, the bonding between xenon and

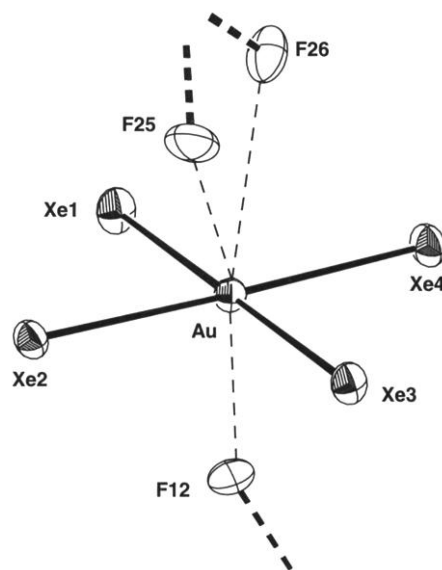


Fig. 1. Crystal structure of the cation AuXe_4^{2+} in $\text{AuXe}_4^{2+}(\text{Sb}_2\text{F}_{11}^-)_2$. Atoms are represented by 50% probability ellipsoids. Shown is the cation with the three closest contacts to the anions. Distances (in pm): Au-Xe1, 273.30(6); Au-Xe2, 274.98(5); Au-Xe3, 272.79(6); Au-Xe4, 274.56(5); Au \dots F12, 267.1(4); Au \dots F26, 295.0(4); Au \dots F25, 315.3(4).

Institut für Chemie, Freie Universität Berlin, Fabeckstrasse 34-36, D-14195 Berlin, Germany.

*To whom correspondence should be addressed. E-mail: seppelt@chemie.fu-berlin.de

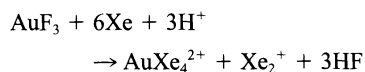
Table 1. Experimental and calculated values for AuXe_4^{2+} .

	Experimental	HF*	Becke3LYP†	MP‡
Au-Xe bond length (pm)	272.8(1)–275.0(1)	289.1	287.1	278.7
Mulliken charges				
Au	–	+0.50	+0.13	+0.34
Xe	–	+0.37	+0.47	+0.41
ΔH (kcal mol ^{–1})				
$\text{Au}^{2+} + 4\text{Xe} \rightarrow \text{AuXe}_4^{2+}$	–	–144	–228	–199

*Hartree-Fock ab initio calculation with a core potential for the inner 60 electrons and a 6s5p3d basis set for Au, and a 4s4p3d1f basis set and a core potential for the inner 46 electrons for Xe (10). †Density functional calculation with the Becke3 method (14) and the correction by Lee, Yang, and Parr (15); same basis set as in the Hartree-Fock calculation. ‡Møller-Plesset second-order calculation; same basis set as in the Hartree-Fock calculation.

gold may not be different from that between xenon and any electronegative main-group element, such as in XeF_2 . Here, a charge transfer of about 0.5 electrons to the electronegative fluorine atom is assumed (12).

During the reduction of Au^{3+} to Au^{2+} and the complexation of Au^{2+} , the extreme Brønsted acidity of the HF/SbF_5 solution is essential. The Au^{3+} ion in fluoride systems is normally present as AuF_4^- , which when protonated, can ultimately lead to $\text{Au}(\text{HF})_4^{3+}$, which has a much higher oxidation potential than AuF_4^- . It can almost be considered as a naked Au^{3+} ion due to the weak basicity of HF. The complexation reaction must be an equilibrium $\text{Au}^{2+}(\text{HF})_n + 4\text{Xe} \rightleftharpoons \text{AuXe}_4^{2+} + n\text{HF}$, which again can only proceed if xenon remains the strongest base in the system. The overall reaction indicates yet again the role of the protons



Green $\text{Xe}_2^+\text{Sb}_4\text{F}_{21}^-$ crystals, which have been fully characterized previously (13), were also detected in the solid reaction mixture at -60°C .

The isolation of the AuXe_4^{2+} cation raises many questions that at present cannot be answered satisfactorily. The main question is, of course, whether this compound remains unique or if this is the first of a series of new complexes. Predictions are difficult because this first compound is also unique in another way: Stoichiometry and structure for a Au^{2+} complex are rare if not entirely new.

References and Notes

1. Bartlett, Proc. R. Chem. Soc. **1962**, 218 (1962).
2. M. B. Simpson, M. Poliakoff, J. J. Turner, W. B. Maier II, J. G. McLaughlin, J. Chem. Soc. Chem. Commun. **1983**, 1355 (1983); B. H. Weiller, J. Am. Chem. Soc. **114**, 10911 (1992); S. A. Fairhurst, J. R. Morton, R. N. Perutz, K. F. Preston, Organometallics **3**, 1389 (1984); J. R. Wells and E. Weitz, J. Am. Chem. Soc. **114**, 2783 (1992); A. W. Ehlers, G. Frenking, E. J. Baerends, Organometallics **16**, 4896 (1997).
3. X.-Z. Sun, D. C. Grills, S. M. Nikiforov, M. Poliakoff, M. W. George, J. Am. Chem. Soc. **119**, 7521 (1997); B. H. Weiller, E. P. Wasserman, R. J. Bergman, C. B. Moore, G. C. Pimentel, J. Am. Chem. Soc. **111**, 8288 (1989); B. H. Weiller, E. P. Wasserman, C. B. Moore, R. B. Bergman, J. Am. Chem. Soc. **115**, 4326 (1993);

- R. H. Schultz et al., J. Am. Chem. Soc. **116**, 7369 (1994); A. A. Bengali, R. H. Schultz, C. B. Moore, R. G. Bergman, J. Am. Chem. Soc. **116**, 9585 (1994); A. A. Bengali, R. G. Bergman, C. B. Moore, J. Am. Chem. Soc. **117**, 3879 (1995); B. K. McNamara, J. S. Yeston, R. G. Bergman, C. B. Moore, J. Am. Chem. Soc. **121**, 6437 (1999).
- D. Schröder, H. Schwarz, J. Hrušák, P. Pykkö, Inorg. Chem. **37**, 624 (1998). For a previous calculation on AuXe^+ and AuXe_2^+ , see also P. Pykkö, J. Am. Chem. Soc. **117**, 2067 (1995).
- C. J. Evans, A. Lesarri, M. C. L. Gerry, J. Am. Chem. Soc. **122**, 6100 (2000).
- L. Graham, O. Graudejus, N. K. Jha, N. Bartlett, Coord. Chem. Rev. **197**, 321 (2000).
- R. Küster and K. Seppelt, Z. Anorg. Allg. Chem. **626**, 236 (2000).
- S. H. Elder, G. M. Lucier, F. J. Hollander, N. Bartlett, J. Am. Chem. Soc. **119**, 1020 (1997).
- $\text{AuXe}_4^{2+}(\text{Sb}_2\text{F}_{11}^-)_2$ crystal parameters: Cell dimen-

sions $a = 794.0 \pm 1$ pm, $b = 917.7 \pm 1$ pm, $c = 1739.1(3)$ pm, $\alpha = 99.539 \pm 5^\circ$, $\beta = 92.640 \pm 4^\circ$, $\gamma = 94.646 \pm 5^\circ$, unit cell volume $V = 1243.4 \times 10^6$ pm³, temperature $T = -120^\circ\text{C}$; space group $P\bar{1}$, number of molecular units in the unit cell $Z = 2$, calculated density $\rho_{\text{calc}} = 3.696$ g/cm³, absorption correction by equalizing symmetry-related reflections with absorption coefficient $\mu = 13.55$ mm^{–1}. MoK α rays with graphite monochromator, 33,456 measured reflections, 8837 unique reflections, max diffraction angle $\theta_{\text{max}} = 31^\circ$, 281 refined parameters, all atoms were refined anisotropically, full least-square matrix refinement, reliability factor $R[F \geq 4\sigma(F)] = 0.039$, weighed reliability factor based on $R^2 wR_2 = 0.099$, weighing scheme $w = 1/\sigma^2[F(o)^2 + (0.0576P)^2 + 1.98P]$, $P = \max[F(o)^2, 0] + 2F_c^2/3$. Further details on the crystal structure determination can be obtained from the Fachinformationszentrum Karlsruhe, 76344 Eggenstein-Leopoldshafen, Germany [Fax: (+49)7247-808-6666; E-mail: crysdta@fiz-karlsruhe.de, accession number CSD 411365].

10. Calculations were done with the program Gaussian 98, Revision E.2 [M. J. Risch et al., Gaussian, Inc., Pittsburgh, PA, 1995]. Basis sets and core potentials were obtained from the Institut für Theoretische Chemie, Universität Stuttgart, Germany.
11. P. Pykkö and J. P. Desclaux, Acc. Chem. Res. **12**, 276 (1979).
12. N. Bartlett and F. O. Sladky, in Comprehensive Inorganic Chemistry, J. C. Bailar and H. J. Emeleus, Eds. (Pergamon, Oxford, 1973), vol. 1, p. 226.
13. T. Drews and K. Seppelt, Angew. Chem. Int. Ed. Engl. **36**, 273 (1997).
14. A. D. Becke, J. Chem. Phys. **98**, 5648 (1993).
15. C. Lee, W. Yang, R. G. Parr, Phys. Rev. B **37**, 785 (1988).

30 June 2000; accepted 31 August 2000

Resurrection of Crushed Magnetization and Chaotic Dynamics in Solution NMR Spectroscopy

Yung-Ya Lin, Natalia Lisitza, Sangdoo Ahn, Warren S. Warren*

We show experimentally and theoretically that two readily observed effects in solution nuclear magnetic resonance (NMR)—radiation damping and the dipolar field—combine to generate bizarre spin dynamics (including chaotic evolution) even with extraordinarily simple sequences. For example, seemingly insignificant residual magnetization after a crusher gradient triggers exponential regrowth of the magnetization, followed by aperiodic turbulent spin motion. The estimated Lyapunov exponent suggests the onset of spatial-temporal chaos and the existence of chaotic attractors. This effect leads to highly irreproducible experimental decays that amplify minor nonuniformities such as temperature gradients. Imaging applications and consequences for other NMR studies are discussed.

Modern high-resolution liquid-state nuclear magnetic resonance (NMR) and magnetic resonance imaging (MRI) experiments often include a complex sequence of radio frequency (RF) pulses for creating and transferring spin

coherence and pulsed-field gradients for coherence pathway selection, rejection, and spatial encoding. The full spin evolution under such sequences is readily calculated even for molecules as large as proteins within the density matrix framework, and such calculations have proven invaluable for pulse sequence optimization and extraction of molecular parameters. Recent work on dipolar field effects in water and other solvents has explained previously

Department of Chemistry, Princeton University, Princeton, NJ 08544, USA.

*To whom correspondence should be addressed. E-mail: wwarren@princeton.edu